

Temperature-dependent angle-resolved photoemission study of the linewidth of surface states of III-V semiconductors

J. Fraxedas, M. K. Kelly, and M. Cardona

Max Planck Institut für Festkörperforschung, Heisenbergstrasse 1, Postfach 80 06 65, D-7000 Stuttgart 80, Federal Republic of Germany

(Received 16 August 1990)

The electron-phonon interaction involving semiconductor surface states is studied on the basis of the temperature dependence of their photoemission linewidths. Measurements of the anion-derived dangling-bond and bridge-bond surface states at critical points for InSb, GaSb, InAs, and GaAs (110) cleaved surfaces were made between 90 and 500 K using high-resolution angle-resolved photoemission spectroscopy. The values of the linewidth determined for $T=0$ K lie between 246 ± 20 and 416 ± 10 meV and are much larger than those found for metal surfaces. In addition to the intrinsic lifetime, there appears to be a contribution to the surface-state linewidth from surface defects such as steps, that are always present to some degree on cleaved surfaces. The localized nature of semiconductor surface states makes them strongly sensitive to such defects. The temperature coefficients lie between 0.18 ± 0.05 and 0.38 ± 0.04 meV/K for the dangling-bond surface states and between 0.07 ± 0.05 and 0.13 ± 0.04 meV/K for the bridge-bond surface states. We also consider the possible effect of plasmon interactions by studying highly doped ($p \sim 10^{19}$ cm $^{-3}$) GaAs samples.

I. INTRODUCTION

The study of the linewidths of optical and electronic transitions in metals and semiconductors is of major interest from the fundamental point of view. The linewidth is related to the imaginary part of the self-energy which is determined by the different many-body processes that contribute to phase relaxation within the excited system, including hole recombination and electron-phonon, electron-electron, and electron-defect interactions. Angle-resolved photoemission spectroscopy (ARPES) is a very useful technique for such studies because it allows the analysis of the band structure at specific points of \mathbf{k} space. In this case the measured linewidth is a convolution of the inverse lifetime of the initial (valence-band) and final (conduction-band) state, the instrumental resolution, and broadening due to interactions of the escaping photoelectron (elastic, such as relaxation of the conservation of the surface-parallel component of the wave vector due to a nonideal surface, or inelastic, such as scattering by plasmons and phonons).¹

At present, however, only a few works have been devoted to the study of the ARPES linewidth in metals and semiconductors and very few of them to its temperature dependence. Room-temperature measurements of bulk critical points in GaAs show values for the initial-state inverse lifetime of approximately 1 eV.² Temperature-dependent analysis of Au (Ref. 3) and of PbS and PbSe (Ref. 4) show a linear dependence of the observed linewidth with temperature. In Ref. 4 the linear temperature coefficient was found to be proportional to the electronic density of initial states for the transitions. This proportionality can be derived from the renormalization of the energy bands due to the electron-phonon interaction.⁵ Most of these measurements were performed at critical points where it is believed that the measured

linewidth is directly associated to the inverse lifetime. A theoretical as well as experimental study of the line shape at critical points assuming a realistic model for the final state (beyond the free-electron approximation), demonstrates asymmetric line shapes due to the non-negligible influence of the electron inelastic scattering on the final-state width.⁶ Measurements of surface states have also been performed for metals at room temperature.⁷⁻⁹ These high-resolution measurements show linewidths of less than 100 meV. To our knowledge only one temperature-dependent study was performed for surface states of metals [Cu (Ref. 9)] and also only one for semiconductor surfaces [InSb (Ref. 1)]. Both works compare the experimental results to the theoretical predictions of Ref. 5. For the (110) surface of InSb it was found that the low-temperature width of surface states was considerably broader than that of metals. It was concluded that differences in intrinsic structure were insufficient to produce this difference, and that the most probable cause of the extra broadening is surface defects.

In the present work we extend these studies to the temperature dependence of the linewidths of the anion-derived dangling bond and bridge bond for selected III-V compound semiconductors at the \bar{X} , \bar{X}' , and \bar{M} points. We call the bridge bond the p -like anion-derived surface state located in the second layer, as mentioned in Ref. 10. Because of the flatness of the bands at these points¹¹ the linewidth is a direct measure of the initial state.¹ Strong similarities are found among the materials under study. We find that the width at low temperature is dominated by broadening due to defects at the surface. The previously mentioned theoretical model is found to be moderately successful in describing temperature coefficient differences among the various features: it assigns them to differences in electronic density of states. We also consider the effects of doping on ARPES line

shapes for the case of GaAs and observe possible effects of scattering of the photoelectron by plasmons.

Section II is concerned with the data interpretation, Sec. III gives a short view of the experimental details and Sec. IV is devoted to the data analysis. Finally, a summary is given in Sec. V.

II. DATA INTERPRETATION

In this section we present the most important expressions for the analysis of the experimental data related to surface states in the frame of the register line formalism and the electron-phonon interaction renormalization. A detailed analysis is found in Ref. 1.

We consider the measured linewidth $\Gamma_{\text{expt}}(T)$ as a convolution of four terms: the combined energy resolution of analyzer and light source Γ_r , the finite angular resolution of the analyzer Γ_θ , and a term Γ_x which contributes to the width if the conservation of the parallel wave-vector component k_x is relaxed due to surface disorder. Finally, the physically most interesting contribution is $\Gamma_e(T)$, which is a combination of the initial- and final-state inverse lifetime widths, $\Gamma_i(T)$ and $\Gamma_f(T)$, respectively. $\Gamma_i(T)$ contains the contribution due to the electron-phonon interaction and $\Gamma_f(T)$ gives the effect of the variation of the electron inelastic mean free path with temperature. For the contributions of the various components to the measured linewidth $\Gamma_{\text{expt}}(T)$ we assume a quadratic addition of the individual linewidth components:

$$\Gamma_{\text{expt}}^2(T) \simeq \Gamma_r^2 + \Gamma_\theta^2 + \Gamma_x^2 + \Gamma_e^2(T). \quad (1)$$

This approximation works well as was confirmed numerically by calculating the convolution directly, although Γ_i and Γ_f are known to be approximately Lorentzians.

Surface states have no dispersion in the initial energy ϵ_i in the perpendicular component of the wave vector k_z so that $v_{iz} = \partial\epsilon_i / \partial k_z = 0$. Furthermore, the bands that correspond to the anion dangling bond and bridge bond have no dispersion in the k_x direction in the vicinity of the critical \bar{X} , \bar{X}' , and \bar{M} points, as was predicted in Ref. 11 and confirmed experimentally in the present work. In this case $v_{ix} \simeq 0$ and $\partial^2\epsilon_i / \partial k_x^2 \simeq 0$. According to Ref. 1, Γ_θ is proportional to v_{ix} for surface states, so that $\Gamma_\theta \simeq 0$. Furthermore, $\Gamma_x \simeq 0$ since Γ_x is defined as the product $|v_{ix} \Delta k_x|$, where Δk_x accounts for the uncertainty in the wave vector k_x due to symmetry breaking.

It can be shown that at critical points the term Γ_e is given by¹

$$\Gamma_e(T) = (1 \pm q)\Gamma_i(T) + q\Gamma_f(T). \quad (2)$$

For surface states q is proportional to $\partial^2\epsilon_i / \partial k_x^2$ (Ref. 1) so that in this case $q \simeq 0$ and thus $\Gamma_e(T) \simeq \Gamma_i(T)$. With the above-mentioned conditions, Eq. (1) reduces to

$$\Gamma_{\text{expt}}^2(T) \simeq \Gamma_r^2 + \Gamma_i^2(T). \quad (3)$$

The electron-phonon model of Ref. 5 allows us to write $\Gamma_i(T)$ as

$$\Gamma_i(T) = \Gamma_i(0) + \frac{2\Sigma_i(0)}{e^{\Theta_i/T} - 1}. \quad (4)$$

$\Sigma_i(0)$ represents the contribution to the linewidth due to the zero-point phonons and $\Gamma_i(0)$ accounts for the linewidth at $T=0$ K. This last term contains $\Sigma_i(0)$ as well as the intrinsic inverse lifetime of the created hole $\Gamma_i^{\text{int}}(0)$ and the contribution Γ_d which arises from the interaction with defects. Θ_i is a heuristic effective average Debye temperature which takes into account the relative contribution of acoustic and optical phonons. Equation (4) follows closely a linear behavior for $T > \Theta_i/e$. In this case

$$\Gamma_i(T) \simeq \Gamma_i(0) + \gamma_i T, \quad (5)$$

where $\gamma_i \simeq 2\Sigma_i(0)/\Theta_i$. According to Ref. 12 $\Sigma_i(0)$ can be expressed as

$$\Sigma_i(0) = \frac{6\pi\hbar}{M_{\text{an}} + M_{\text{cat}}} N_e \frac{\bar{D}^2}{k\Theta_i}. \quad (6)$$

In this expression M_{an} and M_{cat} represent the anion and cation mass, respectively, and k is the Boltzmann constant. N_e is the density of states at the point where the transition starts and \bar{D} is an average electron-phonon deformation potential (in eV/Å units). The factor 6 accounts for the number of phonon branches. Equation (6) has been derived for bulk states but it can be extended to surface states. In the systems that we have studied, $\Gamma_{\text{expt}}^2 \gg \Gamma_r^2$, so that $\Gamma_{\text{expt}}(T) \simeq \Gamma_i(T)$ according to Eq. (3). We thus conclude that

$$\gamma_{\text{expt}} \simeq \gamma_i = 2 \frac{6\pi\hbar k}{M_{\text{an}} + M_{\text{cat}}} N_e \left[\frac{\bar{D}}{k\Theta_i} \right]^2. \quad (7)$$

III. EXPERIMENTAL DETAILS

The temperature-dependent measurements were performed in a Vacuum Generators VG ADES 400 spectrometer with an energy resolution of 70 meV and an angular resolution of $\pm 1^\circ$. The base pressure in the measurement chamber was 1×10^{-10} Torr and only 21.22 eV (HeI) radiation was used. Before cleavage the samples were heated in UHV at 500 K until the initial base pressure was restored, in order to avoid any kind of contamination during the measurements. The maximum temperature was chosen to be 500 K so as to avoid evaporation of the anions [Sb evaporates in the InSb (110) surface at approximately 520 K]. Figure 1 shows the atomic geometry of the (110) surface of the zinc-blende structure [Figs. 1(a) and 1(b)] and the corresponding surface Brillouin zone with the $\bar{\Gamma}$, \bar{X} , \bar{X}' and \bar{M} critical points [Fig. 1(c)]. The \bar{X} point is reached along the $[\bar{1}10]$ and $[\bar{1}1\bar{2}]$ azimuthal directions and the \bar{X}' along $[001]$. The \bar{M} point is reached along the $[\bar{1}11]$ direction. At these points the ARPES intensity ratio between surface and bulk features has a maximum. With the values of k_x [see Fig. 1(c)] and the calculated binding energies from Ref. 11, we obtain the expected value of the emission angle, and thus scan the experimental emission angle until a maximum in the mentioned intensity ratio is found. The semiconductors under study were n -type doped ($n \sim 10^{16} \text{ cm}^{-3}$) InSb, GaSb, InAs, and GaAs and highly p -type doped [$p = (2.2-3.3) \times 10^{19} \text{ cm}^{-3}$] GaAs. No charging

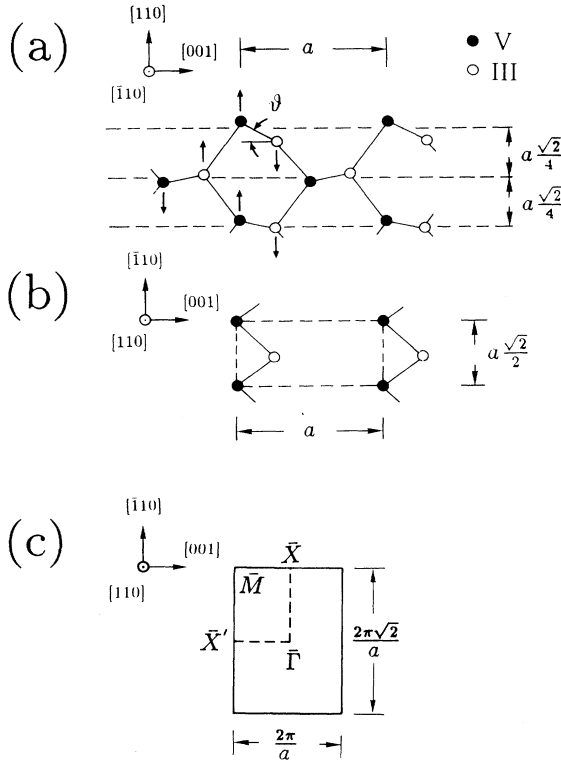


FIG. 1. Relaxed atomic geometry of the (110) face of the III-V zinc-blende semiconductors from (a) side view and (b) top view. The bulk lattice constant is represented by a and the relaxation angle by ϑ . Also shown is the anion-cation chain in the $[\bar{1}10]$ direction. (c) Surface Brillouin zone of the (110) surface with the corresponding critical points.

problems in the temperature range of 90 to 500 K were observed. The linewidths were determined through least-squares fits with combined Gaussian-Lorentzian functions.

IV. RESULTS

In this section we analyze the temperature dependence of the linewidths of surface states of InSb, GaSb, InAs, and GaAs at the critical points \bar{X} , \bar{X}' , and \bar{M} . All the studied features are related to the dangling (DB) and bridge (BB) bonds of the anions Sb and As. Figure 1 shows the atomic geometry of the (110) surface from a side view [Fig. 1(a)] and a top view [Fig. 1(b)]. The side view shows the relaxed form of this surface: the anions are above and the cations below the unrelaxed position, respectively. The angle ϑ that is formed between the anion-cation bond and the unrelaxed position line is called the relaxation angle, which has a value of about 30° for all III-V semiconductors as derived from dynamical low-energy electron diffraction (LEED) and Rutherford backscattering studies as well as from theoretical calculations.¹³

In Fig. 2(a) the measured ARPES spectra of the occupied dangling bonds performed at $T=90$ K at the \bar{X}

point of InSb, GaSb, InAs, and GaAs are shown. Figure 2(b) shows the two corresponding ARPES spectra of InAs at the \bar{X}_{DB} point at the lowest and highest measured temperature. This structure, \bar{X}_{DB} (InAs), shows the strongest variation of the linewidth with temperature. Figure 2(c) shows the experimental values of this linewidth as a function of temperature. Also shown is this fit of the experimental points with Eq. (4). Because of the lack of points below 90 K, the fit is insensitive to the parameter Θ_i . In order to calculate Γ_0 , the linewidth at zero temperature, fits using mean temperatures Θ_i between 50 and 300 K were tested. Ellipsometric measurements on III-V compounds¹⁴ show that $\Theta \sim 300$ K for bulk optical transitions. Since the mean-squared phonon amplitude of the surface atoms at room temperature is expected to be two to three times larger than the corresponding one of the bulk,¹⁵ smaller values of Θ_i for the surface atoms are in principle expected.^{16,17} We thus tested Θ_i in the mentioned temperature range. This range of variation induces differences in the value of Γ_0 of less than ± 6 meV, so we can estimate it reasonably well without precise knowledge of Θ_i . Figure 3(a) shows the ARPES spectra at the \bar{X}'_{DB} point for InSb, GaSb, and InAs and Fig. 3(b) the variation of the linewidth of \bar{X}'_{DB} (InSb) with temperature. The anion bridge bond at \bar{X} has also been measured [see Fig. 4(a)]. The temperature dependence of \bar{X}_{BB} (InAs) is shown in Fig. 4(b). The \bar{X}_{BB} (GaSb), however, can only be observed approximately since at the exact \bar{X}_{BB} point the surface feature overlaps with those of the bulk. The values of the fits for Γ_0 and γ_{expt} , together with the corresponding binding energies ϵ_i and emission angles θ are shown in Table I. In this table values at the \bar{M} point for GaSb and InAs are also included. From the figures, it is obvious that the \bar{X}_{DB} point is the best one for a detailed analysis, since the energy separation from the bulk features is large and the surface-to-volume intensity ratio is also very large. The first property is characteristic of the dangling bonds at the \bar{X}_{DB} point.¹¹

A. Linewidth at $T=0$ K

We analyze here the term Γ_0 and its components. The values of Γ_0 lie between 246 ± 20 and 416 ± 10 meV as can be seen in Table I. Since $\Gamma_0^2 \gg \Gamma_r^2$, the experimental value of Γ_0 can be compared directly to the inverse lifetime $\Gamma_i(0)$ of the initial state. The values of $\Gamma_i(0)$, which agree approximately with estimated values from the room-temperature spectra of the same points,¹⁸ are much larger than reported values for surface states in metals. The Shockley-type sp surface state of Cu has a measured value of $\Gamma_i(0) \leq 100$ meV.⁷⁻⁹ The lowest reported value of $\Gamma_i(0)$ in Cu is 50 meV,^{7,9} which gives a reasonable agreement between available theoretical calculations and experiment. Theoretical estimates of the intrinsic inverse lifetime of the image-potential-induced surface states of metals¹⁹ give values for $\Gamma_i^{\text{int}}(0)$ of less than 20 meV. Analogous calculations have not yet been performed for semiconductors. Values up to 0.4 eV were obtained for $\Gamma(300)$ in metals.²⁰ In this case the above-mentioned sp

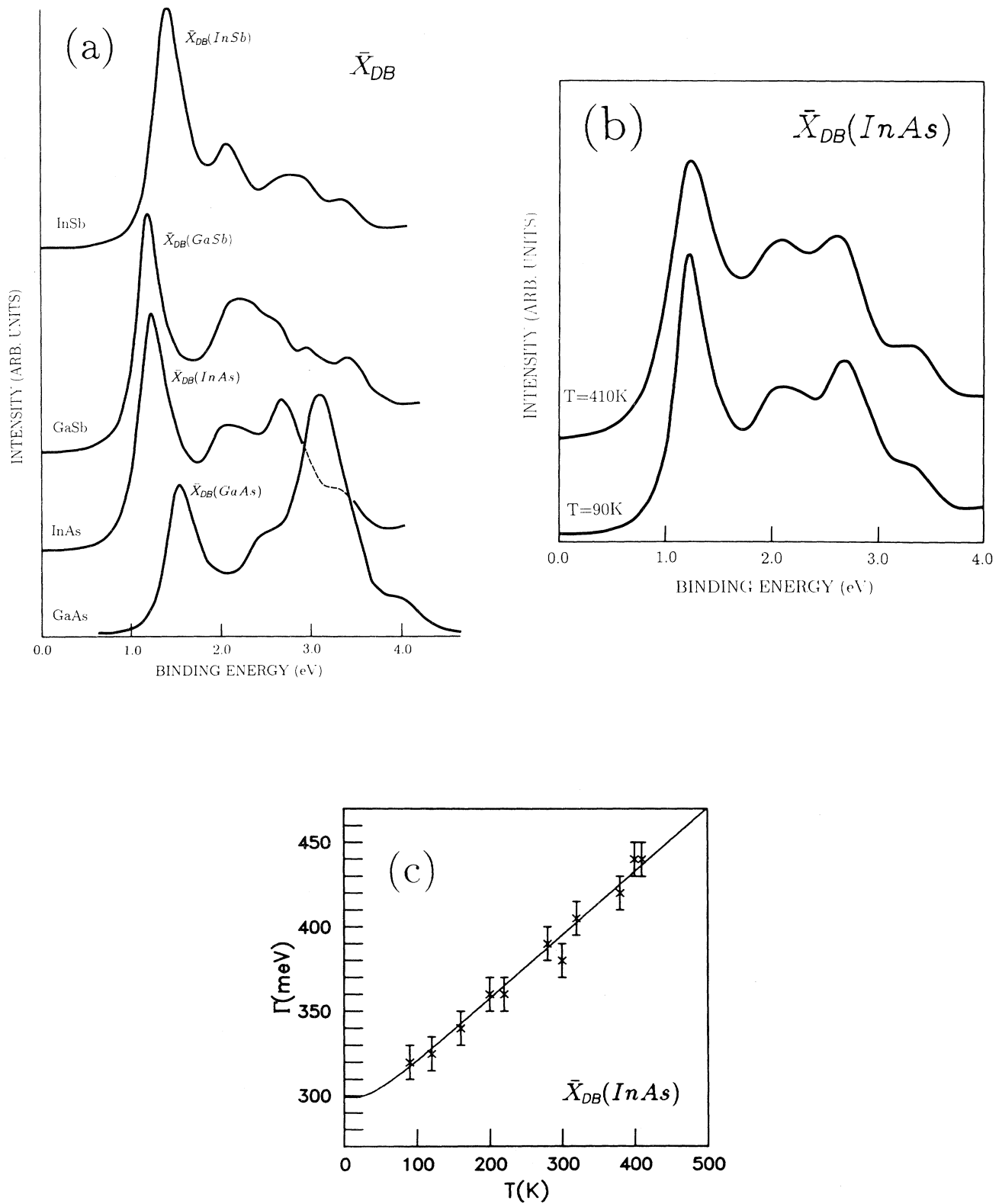


FIG. 2. ARPES spectra of the \bar{X}_{DB} point at $T=90$ K taken with 21.22-eV photons. (a) Spectra of InSb, GaSb, and InAs ($n \sim 10^{16} \text{ cm}^{-3}$) and GaAs ($p \sim 10^{19} \text{ cm}^{-3}$). (b) Comparison of the spectra corresponding to $\bar{X}_{DB}(InAs)$ at $T=90$ K and 410 K. (c) Measured linewidth of $\bar{X}_{DB}(InAs)$ as a function of temperature. This feature shows the strongest temperature coefficient ($\gamma_{\text{expt}}=0.38 \pm 0.04 \text{ meV/K}$).

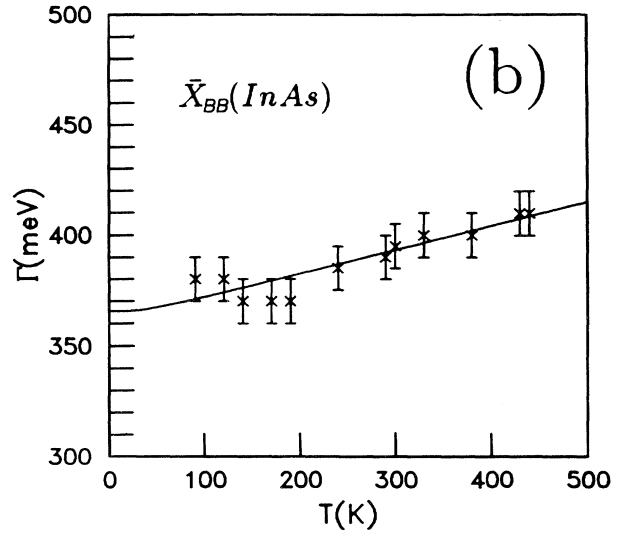
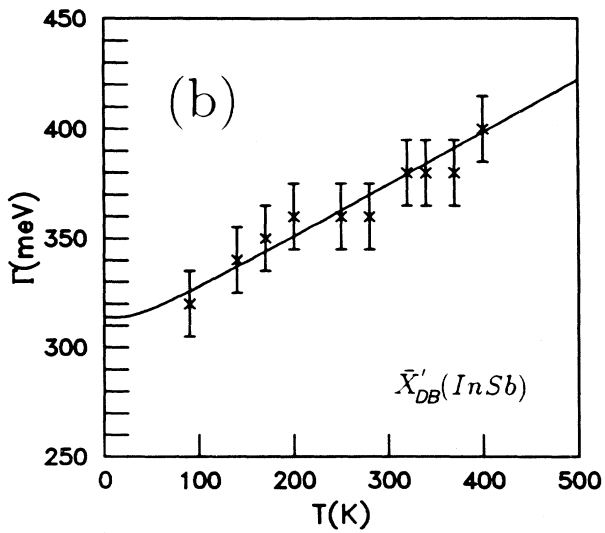
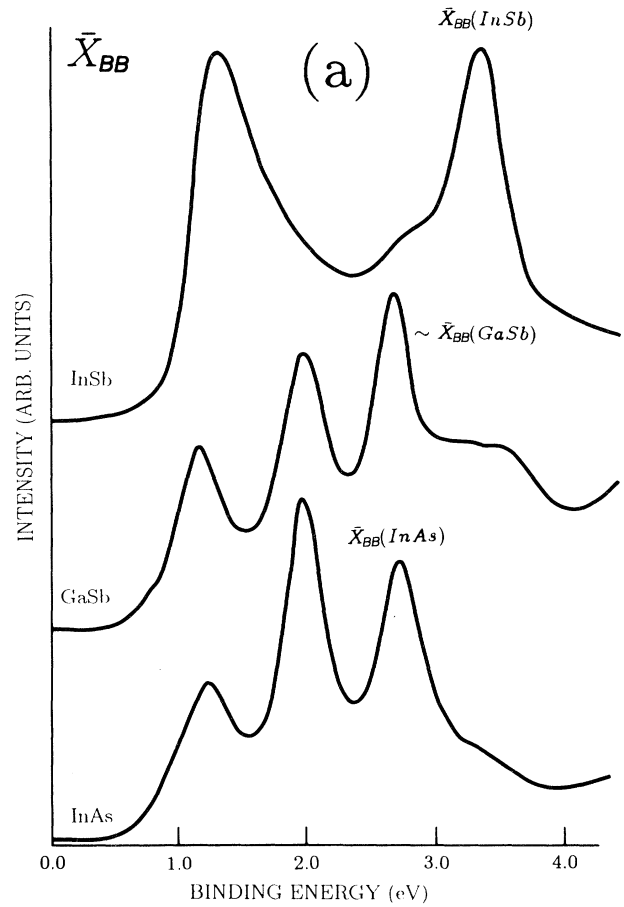
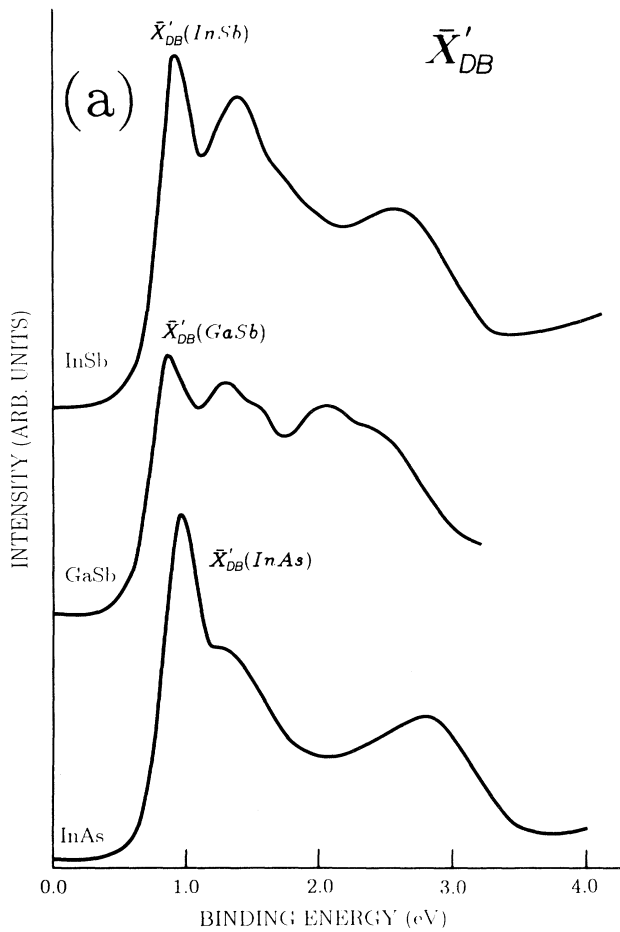


FIG. 3. ARPES spectra of the \bar{X}'_{DB} point at $T=90$ K taken with 21.22-eV photons. (a) Spectra of InSb, GaSb, and InAs ($n \sim 10^{16} \text{ cm}^{-3}$). (b) Measured linewidth of $\bar{X}'_{DB}(\text{InSb})$ as a function of temperature.

FIG. 4. ARPES spectra of the \bar{X}_{BB} point at $T=90$ K taken with 21.22-eV photons. (a) Spectra of InSb, GaSb, and InAs ($n \sim 10^{16} \text{ cm}^{-3}$). (b) Measured linewidth of $\bar{X}_{BB}(\text{InSb})$ as a function of temperature.

TABLE I. Binding energies ϵ_i (referred to the valence-band maximum) and the polar angle θ of selected critical points of the dangling-bond (DB) and bridge-bond (BB) bands together with the linewidth parameters Γ_0 and γ_{expt} for InSb, GaSb, and InAs ($n \sim 10^{16} \text{ cm}^{-3}$). Because of the overlap with the bulk states, \bar{X}_{BB} (GaSb) is not exactly reached. \bar{X}_{DB} (InSb) and \bar{X}_{BB} (InSb) were studied in Ref. 1.

III-V	CP	ϵ_i (eV)	θ (degrees)	Γ_0 (meV)	γ_{expt} (meV/K)
InSb	\bar{X}_{DB}	1.44	20	367 ± 10	0.29 ± 0.04
InSb	\bar{X}_{DB}	0.93	14	312 ± 15	0.24 ± 0.05
InSb	\bar{X}_{BB}	3.33	36	416 ± 10	0.13 ± 0.04
GaSb	\bar{X}_{DB}	1.23	21	265 ± 10	0.33 ± 0.04
GaSb	\bar{X}_{DB}	0.88	15	330 ± 20	0.21 ± 0.05
GaSb	\bar{M}_{DB}	1.03	26	273 ± 20	0.18 ± 0.05
GaSb	$\sim \bar{X}_{\text{BB}}$	2.67	35	270 ± 15	0.07 ± 0.05
InAs	\bar{X}_{DB}	1.23	20	303 ± 10	0.38 ± 0.04
InAs	\bar{X}_{DB}	0.97	12	308 ± 10	0.23 ± 0.04
InAs	\bar{M}_{DB}	1.02	23	246 ± 20	0.28 ± 0.05
InAs	\bar{X}_{BB}	2.70	41	365 ± 10	0.11 ± 0.05

surface state of Cu had a width of approximately 0.25 eV. We believe that the differences arise from insufficient resolution and the quality of the surface, so that the latter values are not representative of Γ_i^{int} .

The calculations of Ref. 19 are performed with hydrogenlike initial states. In this case the wave function has the form $\alpha^{3/2}e^{-\alpha r}$, where r represents the distance to the nuclei and α is a free parameter, with the dimension of an inverse distance, that represents the extension of the wave function. For the dangling bonds this extension is shorter (i.e., α larger) than in metals because the states are strongly localized. As is shown in Ref. 19 the value of $\Gamma_i^{\text{int}}(0)$ increases with increasing α . Hence, according to this model, the value of the intrinsic inverse lifetime in semiconductors should be larger than in metals. For metals the parameter α has a typical value of 0.25. Values between 0.15 and 0.5 give values of $\Gamma_i^{\text{int}}(0)$ between 1 and 28 meV.¹⁹ Thus, although no detailed calculation has been performed for semiconductors, we believe that the measured inverse lifetime is not dominated by hole recombination processes since $\Gamma_i^2(0) \gg [\Gamma_i^{\text{int}}(0)]^2$.

Instead, we believe that the major contribution to the measured inverse lifetime is given by defects at the surface, predominantly steps produced during cleavage. Determination of Γ_x for bulk states by means of ARPES (Ref. 1) suggested that the (110) surfaces of InSb were composed of terraces with a mean length of $110 \pm 60 \text{ \AA}$, or about 17 atomic rows. This value corresponds to a mean value along all the azimuths used in the experiment. In fact, steps are distributed predominantly along specific directions as has been shown by scanning-tunneling-microscopy (STM) measurements on cleaved GaAs.²¹ Although this value was obtained for InSb only, we believe that it can be extended to the other materials since they were cleaved in the same system. The surface bonds in semiconductors are rather localized, so defects at the surface can strongly distort the binding energies. The distortion due to steps will be larger for the atoms lying close to the edge of the terraces than for the atoms in the middle of the terrace so we expect a distribution of ener-

gies from different sites that may appear as a broadening. In metals this effect is smaller because the electrons at the surface are less localized and, consequently, screening will tend to reduce the effect of defects. In addition to steps, distortions of surface states might result from surface stress due to the cleavage. It has been suggested, however, that this stress should be small for cubic materials,²² although the calculations in Ref. 22 were performed using values of bulk parameters as surface parameters, which might introduce an error and consequently a non-negligible contribution to the linewidth.

The values for Γ_0 displayed in Table I correspond to the best surfaces. These surfaces give reproducibly the same values. When the quality of the cleavage is worse we obtain increases of $\Delta\Gamma_0 \sim 100 \text{ meV}$, although the energy dispersion from bulk features is still observable. Since cleavage always results in steps, the only way to measure the intrinsic inverse lifetime from semiconductors with ARPES is to measure *in situ* grown surfaces. The (110) nonpolar surfaces are, however, not usually grown in this way (see nevertheless Ref. 23). The mean terrace length of the (001) surfaces for GaAs is typically 600 \AA .²⁴ We believe that photoemission structures would be sharper for these surfaces, but to our knowledge no such experiments have yet been performed.

In addition to the lifetime of the optical transition and broadening due to defects, ARPES is sensitive to scattering of the photoelectron after the transition. In particular, we consider conduction-band plasmon scattering. For concentrations of free carriers of 10^{16} cm^{-3} , the plasma energy is less than 10 meV. For this small plasma energy, the probability for a photoelectron to lose energy to it is quite large and multiple scattering can occur. The effect of such losses will be an apparent broadening if the instrument does not resolve individual losses.²⁵ High-resolution electron-energy-loss spectroscopy (HREELS) measurements on GaAs,²⁶ however, show that the contribution due to multiple scattering is only about 20 meV for these doping levels.

Thus we find that the measured linewidth of the

dangling-bond and bridge-bond surface states in semiconductors at critical points is dominated by the presence of defects. To a lesser extent, the intrinsic inverse lifetime, surface stress fluctuations, and inelastic scattering can also make a contribution.

B. Temperature coefficients γ_{expt}

We make an analysis based on the parameters of Eq. (7). The experimental values of γ_{expt} are given in Table I. We study first the term N_e , the electronic density of the surface states. For (110) surfaces N_e can be considered, as a first approximation, to be the sum of constant functions of the binding energy. This approximation is suggested by direct inspection of available theoretical calculations.²⁷ In this case we write

$$\begin{aligned} N_e(\varepsilon_i) &= N_e^{\text{DB}}(\varepsilon_i) + N_e^{\text{BB}}(\varepsilon_i) \\ &= \bar{N}_e^{\text{DB}} \Theta_H(\varepsilon_i(\bar{X}_{\text{DB}}) \geq \varepsilon_i) \\ &\quad + \bar{N}_e^{\text{BB}} \Theta_H(\varepsilon_i(\bar{X}_{\text{BB}}) \geq \varepsilon_i \geq \varepsilon_i(\bar{X}'_{\text{DB}})), \end{aligned} \quad (8)$$

where $N_e^{\text{DB}}(\varepsilon_i)$ and $N_e^{\text{BB}}(\varepsilon_i)$ represent the density of states related to the dangling and the bridge bond, respectively. The Heaviside function Θ_H is 1 when the argument of the function is fulfilled and zero otherwise. \bar{N}_e^{DB} and \bar{N}_e^{BB} represent the constant values of N_e^{DB} and N_e^{BB} , respectively. We set \bar{N}_e^{DB} and \bar{N}_e^{BB} inversely proportional to the dangling-bond bandwidth $\varepsilon_{\text{BW}}^{\text{DB}}$ and bridge-bond bandwidth $\varepsilon_{\text{BW}}^{\text{BB}}$, respectively, with a very similar proportionality factor (number of electrons per unit cell). $\varepsilon_{\text{BW}}^{\text{DB}}$ is defined as the energy between $\bar{\Gamma}_{\text{DB}}$ and \bar{X}_{DB} , and $\varepsilon_{\text{BW}}^{\text{BB}}$ between \bar{X}'_{BB} and \bar{X}_{BB} . With these definitions we show in Table II the calculated values for the bandwidths as derived from Ref. 11. We then compare the ratio of the temperature coefficients for linewidths within a given material with the corresponding density of states, in order to study possible correlations.

For InSb the temperature coefficients of the dangling bonds at the \bar{X}_{DB} and \bar{X}'_{DB} points are similar, $\gamma_{\bar{X}_{\text{DB}}} = 0.29 \pm 0.04$ meV/K and $\gamma_{\bar{X}'_{\text{DB}}} = 0.24 \pm 0.05$ meV/K, respectively (see Table I). Since these two points belong to the anion dangling bond they have the same value of \bar{N}_e^{DB} according to our approximation and, correspondingly, they should have the same temperature coefficients, as observed experimentally. Considering the bridge bond, the ratio $\gamma_{\bar{X}_{\text{DB}}} / \gamma_{\bar{X}_{\text{BB}}}$ has a value of 2.23 ($\gamma_{\bar{X}_{\text{BB}}} = 0.13 \pm 0.04$ meV/K) and $\bar{N}_e^{\text{DB}} / \bar{N}_e^{\text{BB}} \simeq \varepsilon_{\text{BW}}^{\text{BB}} / \varepsilon_{\text{BW}}^{\text{DB}}$ equals 2.4, as deduced from Table II. We thus observe

TABLE II. Bandwidth of the dangling-bond band ($\varepsilon_{\text{BW}}^{\text{DB}}$) and of the bridge-bond band ($\varepsilon_{\text{BW}}^{\text{BB}}$) as calculated from Ref. 11 for InSb, GaSb, and InAs. $\varepsilon_{\text{BW}}^{\text{DB}}$ corresponds to the width between $\bar{\Gamma}_{\text{DB}}$ and \bar{X}_{DB} and $\varepsilon_{\text{BW}}^{\text{BB}}$ between \bar{X}'_{BB} and \bar{X}_{BB} .

III-V	$\varepsilon_{\text{BW}}^{\text{DB}}$ (eV)	$\varepsilon_{\text{BW}}^{\text{BB}}$ (eV)
InSb	0.5	1.2
GaSb	0.7	1.4
InAs	0.7	1.6

that for InSb the differences in temperature coefficients can be explained based on the density of states with common values of \bar{D} / Θ_i .

This simple model runs into difficulties for GaSb and InAs. In both cases $\gamma_{\bar{X}_{\text{DB}}}$ is larger than $\gamma_{\bar{X}'_{\text{DB}}}$ and $\gamma_{\bar{M}_{\text{DB}}}$. However the latter two coefficients are very similar, in agreement with the model. The value $\gamma_{\bar{X}_{\text{BB}}}$ of GaSb is not considered since it does not correspond exactly to \bar{X}_{BB} , because at this point there is considerable overlap with bulk states. For InAs, the ratio between $\gamma_{\bar{X}'_{\text{DB}}}$ (or $\gamma_{\bar{M}_{\text{DB}}}$) and $\gamma_{\bar{X}_{\text{DB}}}$ is 2.1, and $\varepsilon_{\text{BW}}^{\text{BB}} / \varepsilon_{\text{BW}}^{\text{DB}} = 2.3$, so that the agreement is again good. We thus observe that this simplified model of the surface density of states accounts for the ratio between temperature coefficients for a given material, except for those at the \bar{X}_{DB} point (InSb is an exception). Theoretical calculations of the surface density of states of AlAs (Ref. 28) show a strong maximum around the \bar{X}_{DB} point. The ratio between the average density of states and this maximum is around 0.6. This behavior is also approximately observed in the calculations for GaAs (Ref. 27) so we believe that it can be extended to the III-V semiconductors used in the present work. This value is also found between $\gamma_{\bar{X}_{\text{DB}}}$ and $\gamma_{\bar{X}'_{\text{DB}}}$ (or $\gamma_{\bar{M}_{\text{DB}}}$) for GaSb and InAs, possibly explaining the discrepancies. The same kind of analysis can be performed for the different temperature coefficients of different materials. These coefficients are very similar for InSb, GaSb, and InAs as well as for GaAs [in this case only $\gamma_{\bar{X}_{\text{DB}}} (= 0.33$ meV/K) was measured]. Note, however, the discrepancy at \bar{M}_{DB} for InAs and GaSb. We thus conclude that the factor

$$\frac{1}{M_{\text{an}} + M_{\text{cat}}} \left[\frac{D}{k \Theta_i} \right]^2$$

does not show strong variations among the different states or materials in most cases and that the density of states accounts for most of the variation in the temperature coefficients.

We consider next the expression D / Θ in more detail. This could, in principle, be calculated if the surface phonon density of states and the corresponding coupling strengths were known. However, only limited information is available,²⁹ so that we consider, as a first approximation, a limited part of the electron-lattice interaction. In particular, it is known that the relaxation of the surface denoted by the parameter ϑ , has a strong effect on the energy of the surface states ε_i , causing the dangling-bond states to move out of the bulk gap.³⁰ [Note, however, that these states have been observed to remain in the gap for two of the materials: GaSb (Ref. 31) and InSb (Ref. 10)]. Recently a vibrational mode has been observed in GaAs by inelastic scattering of He atoms at an energy of 10 meV.³² This mode has been attributed to a bond-length-conserving libration of the anion-cation chain within the $[\bar{1}10]$ direction similar to the rotation corresponding to the relaxation³³ [see Fig. 1(b)]. A similar mode has been also observed in the Si(111)-(2 × 1) sur-

face with an energy of 10.5 meV,³⁴ which is associated with the oscillation of the reconstruction-induced tilted chains.³⁵ The fact that both modes have almost the same value is a consequence of the similarity of the relaxed (110) surfaces of the III-V and the reconstructed (111)-(2×1) of Si. This mode has also a value around 10 meV for many III-V and II-VI semiconductors, according to theoretical calculations of Refs. 33 and 36. Because of the similarity between this mode and the relaxation, we try to analyze its coupling constants (deformation potential) to electronic states. The effect of similar modes on surface spectra for Si has earlier been investigated.^{37,38}

To consider the effect on linewidth of coupling to this mode, we estimate the deformation potential using theoretical calculations of the variation of the binding energy ε_i as a function of the relaxation angle ϑ [Fig. 2(a) from Ref. 30]. These estimates give a minimum of ε_i around $\vartheta = 27^\circ$, whereas total-energy minimization calculations deliver values of 31° (Ref. 39) and LEED gives 29° .³³ We thus approximate the deformation potential as the slope of $\varepsilon_i(\vartheta)$ at 31° . After transforming ϑ into an atomic displacement it results in $D \sim 1$ eV/Å, which is smaller than calculated deformation potentials of bulk intervalley transitions¹⁷ for which $\bar{D} \sim 3$ eV/Å. If we use the experimental value of 29° , the coupling is even weaker. Since the energy of this mode (10 meV) corresponds to a temperature of 120 K compared to the bulk (~ 300 K), the ratio \bar{D}/Θ_i , should be close to the average. We thus conclude that the effect of the bond-length-conserving libration of the anion-cation chain on the temperature dependence of the ARPES peaks is average to weak. This conclusion differs from an analysis of Si(111)-(2×1) surfaces,^{37,38} which interpret the strong temperature dependence of the width of the dangling-bond transitions as due to a strong coupling to the Einstein mode at 10.5 meV. We note that the analyses performed in these references are based on models for electron-phonon coupling, other than band renormalization, which give $T^{1/2}$ rather than linear temperature dependence of the width: frozen-phonon mode³⁷ or localized transitions.³⁸ However, the qualitative difference in our conclusions appears to be due to differences in the Si(111)-(2×1) and the GaAs(110) surfaces. The seemingly surprising weak deformation potential for this mode, despite the strong effect of relaxation, is explainable because the dangling bond state has minimum energy at nearly the same angle as the total energy, giving thus a small value of $\partial\varepsilon_i/\partial\vartheta$ at the equilibrium position. This value is not so small for Si(111) ($D \sim 4$ eV/Å).³⁷

Assuming then that no particular subset of phonons has a dominant contribution, we estimate Θ_i for the dangling bond of GaAs. For this purpose we take the experimental value of γ_i ($=0.33$ meV/K), the calculated density of states as derived from Ref. 11 ($\bar{N}_e^{DB} \sim 1/0.5$ eV⁻¹) and we assume D to have similar values as for bulk states ($D \sim 3$ eV/Å), as suggested in Ref. 40. By using Eq. (7) for all the phonon branches (with the factor 6), we obtain $\Theta_i \sim 400$ K ($\hbar\omega \sim 36$ meV), a value somewhat larger than the accepted 300 K for bulk transitions. It thus appears that the temperature dependence of the widths is high primarily due to the high density of states. For a more

detailed analysis, more information about coupling strengths and density of phonon and electron states is needed.

C. Influence of doping on the line shape of \bar{X}_{DB} (GaAs)

Together with the room-temperature measurements of the \bar{X}_{DB} point of GaAs for lightly doped samples ($n \sim 10^{16}$ cm⁻³), spectra at the same point for heavily doped samples ($p \sim 10^{19}$ cm⁻³) were also taken in order to study the influence of the doping on the line shape. The measured spectra are shown in Fig. 5(a). Since the

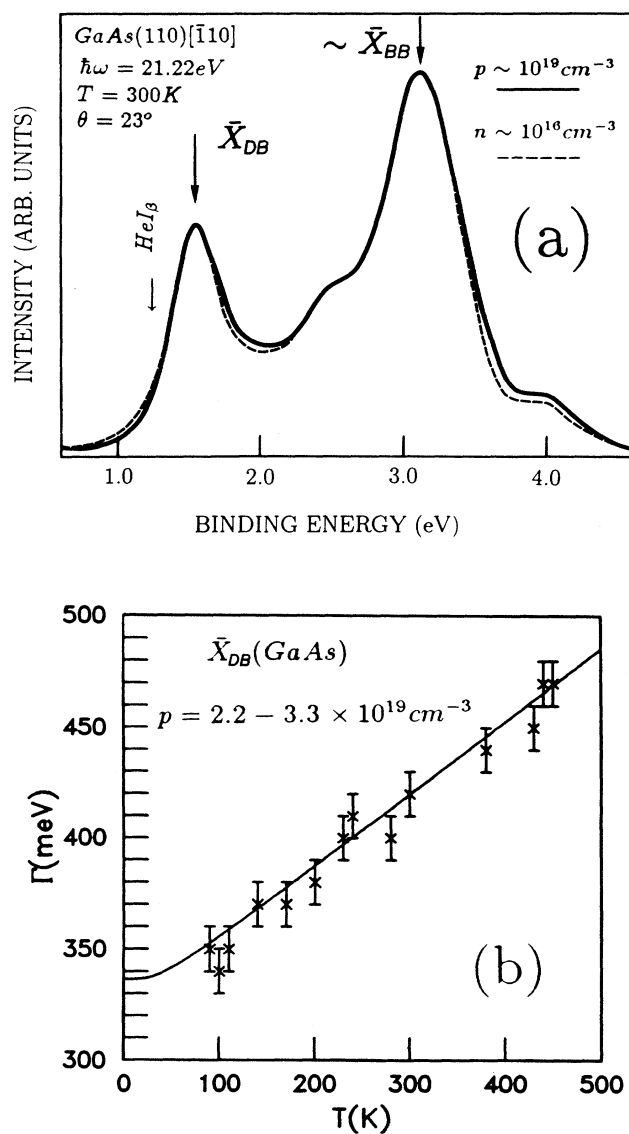


FIG. 5. (a) Comparison of the ARPES spectra of the \bar{X}_{DB} point for heavily doped ($p \sim 10^{19}$ cm⁻³, solid line) and lightly doped ($n \sim 10^{16}$ cm⁻³, dashed line) GaAs. The position of the $\sim \bar{X}_{BB}$ point excited with the HeI β satellite (23.09 eV) is also shown. (b) Measured linewidth for \bar{X}_{DB} (GaAs) as a function of temperature for the heavily doped sample.

difference due to doping is small, and in general different surfaces have different defect densities, we confirmed reproducibility by measuring many surfaces for both the heavily and lightly doped samples. The spectra of Fig. 5(a) show typical spectra that reproducibly have the same line shape. The two spectra have been shifted with respect to each other by 0.89 eV in order to line up the peaks, since the two types of doped samples have different Fermi levels. Thus the figure can only be used for line-shape studies and not for frequency shifts. In addition, the relative intensities of the curves, which for different cleaves are generally arbitrary, have been normalized to give equal peak heights for the bridge bond.

The increased intensity for the heavily doped sample on the low kinetic energy (high binding energy) side of the peaks may be due to inelastic scattering by free carriers (plasmons). The plasma frequencies of the free carriers are given by⁴¹

$$\omega_p^2 = \omega_s^2 \frac{\epsilon_0 + 1}{\epsilon_0} = \frac{4\pi N e^2}{m_{\text{eff}} \epsilon_0}, \quad (9)$$

where ω_p and ω_s represent the bulk and surface plasma frequencies, respectively, ϵ_0 the static dielectric constant, m_{eff} the effective mass, and N the carrier concentration. Using Eq. (9) with $m_{\text{eff}} = 0.067m_e$ and $\epsilon_0 = 12.85$ (Ref. 26) and $N = n \sim 10^{16} \text{ cm}^{-3}$, we obtained the above-mentioned value $\hbar\omega_p \sim 10 \text{ meV}$. For $N = p \sim 10^{19} \text{ cm}^{-3}$ and $m_{\text{eff}} = 0.5m_e$,⁴² we obtain $\hbar\omega_p \sim 80 \text{ meV}$ for the same value of ϵ_0 . This last value is no longer small compared to our resolution and such losses may be responsible for the asymmetric broadening. When, as in this case, the loss is comparable to the peak width, the spectrum is not very sensitive to loss energy so we do not attempt a detailed fit. We note, however, that the interaction with such plasmons is probably strong enough to cause this effect as deduced from comparison with HREELS results.⁴³ Because $\epsilon_0 \gg 1$ it follows that $\omega_p \simeq \omega_s$, so that no distinction between bulk and surface plasmons is considered. We would however need another explanation for the higher intensity of the undoped sample in the high-kinetic-energy (low-binding-energy) side of \bar{X}_{DB} . One possible reason is that the inhomogeneities of the Fermi-level position on the surface due to defects are less effectively screened for the low carrier concentration but we are unable to draw a firm conclusion.

In Fig. 5(a) the position of the \bar{X}_{BB} point expected for excitation with the He I $_{\beta}$ (23.09 eV) satellite is also shown. Since the contribution of this satellite in our experimental setup is very small (around 4%) and since the spectra are very similar, this contribution is neglected.

In addition to the plasmon scattering, there could be an effect on the initial-state lifetime due to doping. The temperature dependence of the linewidth of the \bar{X}_{DB} point for the highly doped sample is shown in Fig. 5(b). We first consider the term Γ_0 . In addition to the previously mentioned contribution of surface defects, the high concentration of ionized dopants may contribute to the linewidth. Determining the full width at half maximum (FWHM) by doubling the HWHM on the lower-binding-

energy side (in order to avoid the asymmetric effect of the plasmon losses), we obtain $\Gamma_0 = 330 \pm 10 \text{ meV}$ for both free-carrier concentrations, so that no measurable difference was observed. Ellipsometric measurements of the E_1 and E_2 gaps of Si (Ref. 44) and GaAs (Ref. 45), show that the intrinsic inverse lifetime increases with the free-carrier concentration according to an N^{α_D} law, where N represents the doping and α_D an exponential factor. This expression can be derived in the framework of the renormalization of energy bands due to interaction of electrons with impurities.⁴⁴ The exponential α_D has a typical value ~ 0.5 for the above-mentioned optical transitions. The measured changes between pure materials and sample with $N \sim 10^{20} \text{ cm}^{-3}$ are typically less than 30 meV, differences that cannot be observed with our photoemission system. We conclude that the influence of the free carriers on the linewidth at zero temperature is small compared to that of surface defects.

The temperature dependence of Γ_i for the $p \sim 10^{19} \text{ cm}^{-3}$ sample is shown in Fig. 5(b). The corresponding temperature coefficient is $\gamma_i = 0.33 \pm 0.04 \text{ meV/K}$. Since this is similar to the values for the low-doped samples, we conclude that the electron-phonon coupling discussed earlier dominates the temperature dependence of the lifetime broadening as compared to electron plasmon coupling which would be significantly affected by the carrier density. Thus the coupling to the 10-meV plasmons of the slightly doped materials must be weak.

V. SUMMARY

We have presented a study of the temperature dependence of the photoemission linewidth of the dangling and bridge bonds at critical points of InSb, GaSb, InAs, and GaAs (110) surfaces. The linewidth at zero temperature is dominated by the presence of defects at the surface due to cleavage, since they distort the rather localized surface states. To a lesser extent, the intrinsic inverse lifetime contributes to this term. The effect of multiple inelastic scattering and surface stress is considerably smaller. The temperature coefficients have been compared to a model based on the renormalization of the energy bands by the electron-phonon interaction. These coefficients are functions of the density of states at the point where the transitions occur and of an average effective Debye temperature. We have proposed a simple approximation for the density of surface states which separates the contributions from the dangling- and bridge-bond bands. This model allows the comparison of different temperature coefficients for a given material as well as for different materials; it works reasonably well except at the \bar{X}_{DB} point. It appears that differences in the coefficients compared with the bulk can also be explained as primarily due to differences in electronic density of states.

Measurements of the \bar{X}_{DB} point of GaAs with heavily and lightly doped samples suggest resolvable plasmon loss at high carrier density, although no quantitative estimates can be made. The influence of impurities to the linewidth was found to be negligible and the temperature

coefficient of the heavily doped sample was shown to be also dominated by the electron-phonon interaction.

More detailed analysis will require characterization of the same surfaces used for the ARPES measurements with complementary techniques such as HREELS and LEED in order to better understand the effect of surface defects and inelastic scattering. ARPES measurements down to 20 K are also desirable. Calculations of both the density of surface electronic and phonon states will be also needed, in order to compare the temperature coefficients of different compounds. Systematic studies of

the ARPES spectra for different carrier concentrations are also necessary.

ACKNOWLEDGMENTS

J. Fraxedas would like to thank the Directorate General for Science, Research and Development (European Community Brussels) and M. Kelly the Alexander von Humboldt Foundation (Bonn, Germany) for financial support. We are grateful to L. Ley and to F. Yndurain for fruitful discussions.

- ¹J. Fraxedas, H. J. Trodahl, S. Gopalan, L. Ley, and M. Cardona, *Phys. Rev. B* **41**, 10 068 (1990).
- ²T. C. Chiang, J. A. Knapp, M. Aono, and D. E. Eastman, *Phys. Rev. B* **21**, 3513 (1980).
- ³P. Heimann and H. Neddermeyer, *Solid State Commun.* **26**, 279 (1978).
- ⁴T. Grandke, M. Cardona, and L. Ley, *Solid State Commun.* **32**, 353 (1979).
- ⁵P. B. Allen and M. Cardona, *Phys. Rev. B* **27**, 4760 (1983).
- ⁶J. Fraxedas, H. J. Trodahl, and L. Ley, *Phys. Scr.* **41**, 905 (1990).
- ⁷S. D. Kevan and D. A. Shirley, *Phys. Rev. B* **22**, 542 (1980).
- ⁸S. Kevan, *Phys. Rev. B* **33**, 4364 (1986).
- ⁹G. Staperfeld (unpublished).
- ¹⁰R. Manzke and M. Skibowski, *Phys. Scr.* **31**, 87 (1990).
- ¹¹C. Mailhot, C. B. Duke, and D. J. Chadi, *Phys. Rev. B* **31**, 2213 (1985).
- ¹²P. Lautenschlager, P. B. Allen, and M. Cardona, *Phys. Rev. B* **33**, 5501 (1986).
- ¹³G. V. Hansson and R. I. G. Uhrberg, *Surf. Sci. Rep.* **9**, 197 (1988).
- ¹⁴S. Logothetidis, L. Viña, and M. Cardona, *Phys. Rev. B* **31**, 947 (1985); P. Lautenschlager, M. Garriga, L. Viña, and M. Cardona, *ibid.* **36**, 4821 (1987).
- ¹⁵N. J. Shevchik, *Phys. Rev. B* **16**, 3428 (1977).
- ¹⁶S. Zollner, S. Gopalan, M. Garriga, J. Humlíček, and M. Cardona, in *Proceedings of the 19th International Conference on the Physics of Semiconductors, Warsaw, 1988*, edited by W. Zawadzki (Institute of Physics/Polish Academy of Sciences, Warsaw, 1988).
- ¹⁷S. Zollner, S. Gopalan, and M. Cardona, *Appl. Phys. Lett.* **54**, 614 (1989).
- ¹⁸H. Carstensen, R. Claessen, R. Manzke, and M. Skibowski, *Phys. Rev. B* **41**, 9880 (1990).
- ¹⁹P. M. Echenique, F. Flores, and F. Sols, *Phys. Rev. Lett.* **55**, 2348 (1985).
- ²⁰E. W. Plummer and W. Eberhardt, *Phys. Rev. B* **20**, 1444 (1979).
- ²¹R. Möller, R. Coenen, B. Koslowski, and M. Rauscher, *Surf. Sci.* **217**, 289 (1989).
- ²²R. G. Lindford, L. A. Mitchel, C. Osgood, and M. P. Williams, *Surf. Sci.* **219**, 341 (1989).
- ²³Z. V. Popović, M. Cardona, E. Richter, D. Strauch, L. Tapfer, and K. Ploog, *Phys. Rev. B* **40**, 3040 (1989), and references therein.
- ²⁴P. R. Pukite, C. S. Lent, and P. I. Cohen, *Surf. Sci.* **161**, 39 (1985).
- ²⁵H. Ibach and D. L. Mills, *Electron Energy Loss Spectroscopy and Surface Vibrations* (Academic, New York, 1982).
- ²⁶L. H. Dubois, B. R. Zegarski, and B. N. J. Persson, *Phys. Rev. B* **35**, 9128 (1987).
- ²⁷D. J. Chadi, *Phys. Rev. B* **18**, 1800 (1978).
- ²⁸N. E. Christensen (unpublished).
- ²⁹V. Bortolani, F. Nizzoli, and G. Santoro, *Phys. Rev. Lett.* **41**, 39 (1978).
- ³⁰C. Mailhot, C. B. Duke, and Y. C. Chang, *Phys. Rev. B* **30**, 1109 (1984).
- ³¹R. Manzke, H. P. Barnscheidt, C. Janowitz, and M. Skibowski, *Phys. Rev. Lett.* **58**, 610 (1987).
- ³²U. Harten and J. P. Toennies, *Europhys. Lett.* **4**, 833 (1987).
- ³³C. B. Duke and Y. R. Wang, *J. Vac. Sci. Technol. B* **7**, 1027 (1989).
- ³⁴U. Harten, J. P. Toennies, and Ch. Wöll, *Phys. Rev. Lett.* **57**, 2947 (1986).
- ³⁵L. Miglio, P. Santini, P. Ruggerone, and G. Benedek, *Phys. Rev. Lett.* **62**, 3070 (1989).
- ³⁶Y. R. Wang and C. B. Duke, *Surf. Sci.* **205**, L755 (1988).
- ³⁷M. A. Olmstead and D. J. Chadi, *Phys. Rev. B* **33**, 8402 (1986).
- ³⁸F. Ciccacci, S. Selci, G. Chiarotti, and P. Chiaradia, *Phys. Rev. Lett.* **56**, 2411 (1986).
- ³⁹A. C. Ferraz and G. P. Srivastava, *Surf. Sci.* **182**, 161 (1987).
- ⁴⁰C. Tejedor, F. Flores, and E. Louis, *J. Phys. C* **19**, 543 (1986).
- ⁴¹T. Inaoka, D. M. News, and R. G. Egdell, *Surf. Sci.* **186**, 290 (1987).
- ⁴²J. I. Pankove, *Optical Processes in Semiconductors* (Dover, New York, 1971).
- ⁴³Y. Chen, S. Nannarone, J. Schaefer, J. C. Hermanson, and G. J. Lapeyre, *Phys. Rev. B* **39**, 7653 (1989).
- ⁴⁴L. Viña and M. Cardona, *Phys. Rev. B* **29**, 6739 (1984).
- ⁴⁵F. Lukeš (unpublished).